

Shape selectivity for alkane hydroxylation with a new class of phosphonate-based heterogenised manganese porphyrins

David Deniaud,^a Georgios A. Spyroulias,^b Jean-François Bartoli,^b Pierrette Battioni,^b Daniel Mansuy,^b Catherine Pinel,^c Fabrice Odobel^a and Bruno Bujoli^{*a}

^a Laboratoire de Synthèse Organique, (CNRS UMR 6513), 2 rue de la Houssinière, BP 92203, 44322 Nantes cedex 03, France

^b Laboratoire de Chimie et Biochimie Pharmacologiques et Toxicologiques (CNRS URA 400), Université René Descartes, 45 rue des Saints-Pères, 75270 Paris cedex 06, France

^c Institut de Recherches sur la Catalyse (CNRS UPR 5401), 2 avenue Albert Einstein, 69626 Villeurbanne cedex, France

Four new manganese(III) porphyrins, heterogenised as insoluble zinc phosphonates, exhibit behaviour markedly different from their homogeneous counterparts in the competitive hydroxylation of alkane mixtures (*i.e.*, cyclododecane–cyclohexane), using iodosylbenzene as the oxidant. The cyclohexanol : cyclododecanol ratio can be increased by as much as five, owing to shape selectivity effects imposed by the phosphonate support.

Sélectivité de forme pour l'hydroxylation d'alcane, catalysée par des porphyrines de manganèse hétérogénéisées sous forme de phosphonates de zinc. Une série de quatre tétraarylporphyrines de manganèse(III) hétérogénéisées sous forme de phosphonates de zinc insolubles, testées pour l'hydroxylation compétitive de mélanges d'alcane (par exemple, cyclododécane–cyclohexane) par l'iodosobenzène, montrent un comportement très différent de celui de leurs homologues non supportés en milieu homogène. Le rapport cyclohexanol : cyclododécanol peut augmenter d'un facteur allant jusqu'à cinq, sous l'effet d'une sélectivité de forme induite par le support phosphonate.

In hybrid materials such as phosphonates, in which organic and inorganic units are combined, strong interactions inevitably exist in solution between the organic and inorganic precursors. These play a significant role during the self-assembly of the phosphonate network, which results from the reaction of an RPO_3H_2 (R = organic substituent) phosphonic acid with a metal salt, with formation of metal–oxygen bonds.¹ Among the parameters having a strong influence on the structure of phosphonates, the nature of the organic moiety bound to phosphorus is certainly the most important; thus, we have shown in several studies how the inorganic framework has to adapt to the characteristics of the organic units (size, functional groups, flexibility, polarity, *etc.*).²

Until now, the chemistry of phosphonates has been roughly limited to the use of relatively simple phosphonic acids, but we have recently investigated the possibility of immobilising catalytic complexes as insoluble metal phosphonates. In addition to the facilitated recovery of solid catalysts from the reaction media, an additional benefit in the heterogenisation of homogeneous catalysts is the potential increase in product selectivity, resulting from steric constraints imposed by the support material. In some cases (*i.e.*, in zeolites or MCM-41)³ the catalytic reaction takes place in confined spaces, leading to selectivities (regio-, stereo- and chemoselectivities) different from those observed under homogeneous conditions.

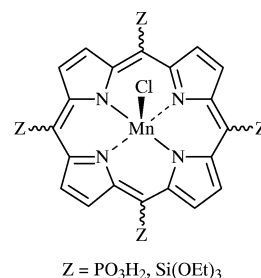
Our first attempts were focused on the covalent immobilisation of metalloporphyrin catalysts that mimic cytochrome P450. Our strategy for this purpose was new and consisted in the functionalisation of the porphyrin complex with 'polymerisable moieties' (Scheme 1, $\text{Z} = \text{PO}_3\text{H}_2$)⁴ that subsequently allow the construction of the metal phosphonate network, in which the metalloporphyrin is incorporated [a similar approach was developed with $\text{Z} = \text{Si}(\text{OEt})_3$; the inorganic host framework in that case is silica].⁵ For both series,

the corresponding supported metalloporphyrins have proved to be efficient catalysts for alkene epoxidation and alkane hydroxylation.

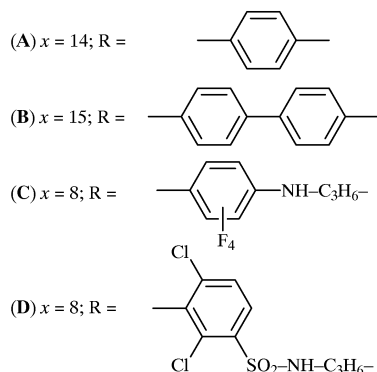
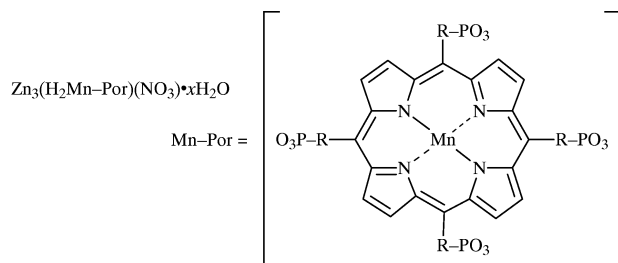
As mentioned previously, the geometry of the organic precursor is expected to influence greatly the structural features of these phosphonate-based supported porphyrins, as well as their catalytic properties. It was therefore of interest to determine if the nature of the spacer separating the porphyrin core and the polymerisable PO_3H_2 moieties had significant effects on the physical and chemical properties of the resulting immobilised porphyrins.

Results

For this study, four new manganese(III) porphyrin precursors **1A–1D**, tetrafunctionalised by PO_3Et_2 groups separated from the porphyrinic macrocycle by variable linkers (see **R** in Scheme 2), were prepared. After conversion of the phosphonate ester groups into the acidic form, their heterogenisation as zinc phosphonates (**A–D**, Scheme 2) was



Scheme 1 Functionalisation of metalloporphyrins for their heterogenisation as metal phosphonates or silsesquioxanes



Scheme 2 Schematic representation of the immobilised manganese porphyrins A–D

performed by reaction with an excess of zinc nitrate in refluxing methanol for 5 days. From chemical analyses a similar general formula was found for compounds A–D: $\text{Zn}_3(\text{H}_2\text{Mn-Por})(\text{NO}_3) \cdot x\text{H}_2\text{O}$ (Scheme 2), the water content depending on the nature of the precursor. As a consequence of the rather mild polymerisation conditions used, no noticeable alteration of the porphyrins was observed.

(i) The main characteristic infrared bands of the porphyrinic precursors are present at the same frequencies in the corresponding zinc phosphonates, except for the PO_3 region, giving evidence of the ‘inorganic polymerisation’ taking place at the phosphonic acid units.

(ii) The UV/VIS data show nearly identical absorptions (particularly for the Soret band) for the hybrid materials and the corresponding precursors (i.e., 468 nm for A and 466 nm for 1A, Table 1), thus indicating that Mn^{III} –porphyrin sites are still present in A–D.

(iii) Moreover, used as a comparative structural tool, X-ray absorption near edge structure (XANES) spectroscopy agrees well with the location of the manganese atoms in the porphyrin cage; compounds A–D and their precursors 1A–1D have superimposable X-ray absorption Mn K-edge spectra, comparable to that previously observed in the literature for Mn^{III} porphyrins.⁶

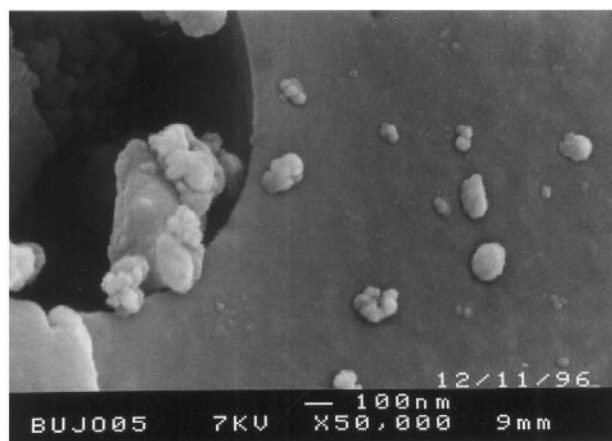
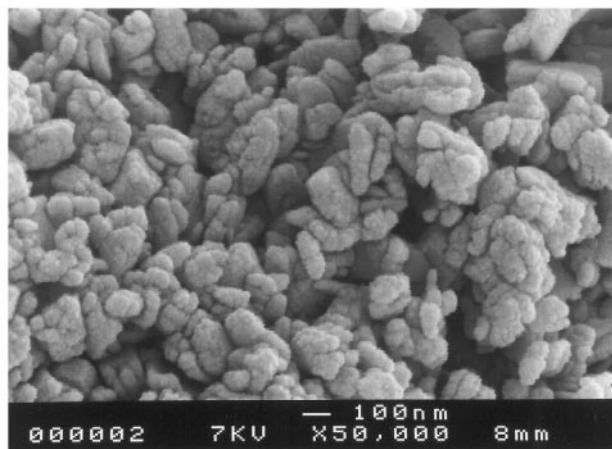


Fig. 1 SEM (magnified 50000 times) of the supported porphyrins A (top) and C (bottom)

(iv) For each of the four heterogenized porphyrins, ^{31}P MAS NMR experiments give one well-defined signal for the phosphorus atoms (consistent with the presence of relatively well-organized and homogeneous solids, Table 1), with chemical shifts consistent with those observed for zinc aryl- (15–17 ppm for A and B) and alkyl-phosphonates (ca. 29 ppm for C and D).

One interesting feature is that high surface areas are observed for the first two porphyrins A and B (A: $320 \text{ m}^2 \text{ g}^{-1}$; B: $560 \text{ m}^2 \text{ g}^{-1}$), while very low values (around $5 \text{ m}^2 \text{ g}^{-1}$) are measured for the last two, C and D. These observations are in

Table 1 Experimental data for the supported metalloporphyrins

	A ^a	A ^b	B ^a	C ^a	D ^a
TGA	16.3	16.5	15.0	7.8	6.5
% water loss	(16.9) ^c		(14.9) ^c	(7.6) ^c	(6.7) ^c
BET surface area/ $\text{m}^2 \text{ g}^{-1}$	320	75	560	5	5
Microporous surface area/ $\text{m}^2 \text{ g}^{-1}$	250	10	470		
^{31}P MAS NMR δ_{iso} ppm	17.5	17.7	15.1	28.9	29.2
UV/VIS /nm	468 (Soret), 522, 573, 610 [466 (Soret), 518, 568, 606] ^d		480 (Soret), 588, 628 [479 (Soret), 584, 621] ^d	460 (Soret), 505, 561, 677 [462 (Soret), 557, 679] ^d	468 (Soret), 572 [467 (Soret), 565, 661] ^d

^a As defined in Scheme 2. Standard preparation time is 5 days. ^b Same protocol as for A, with a preparation time of 8 h. ^c Calculated value.

^d Values for the corresponding molecular precursor 1A–1D.

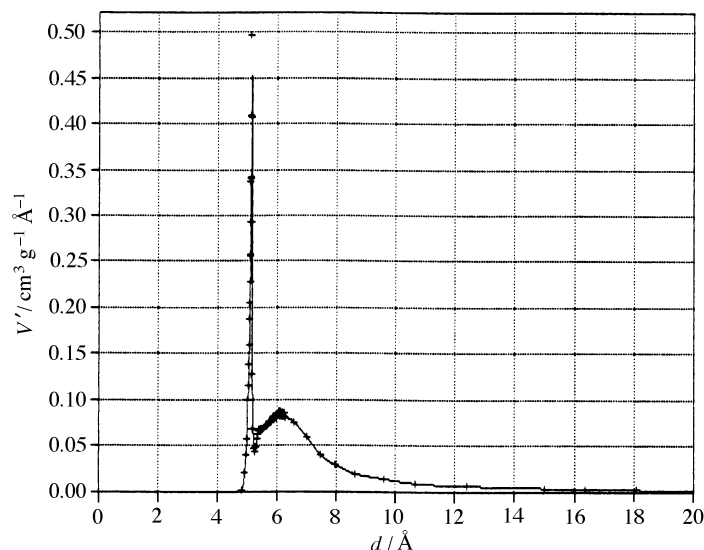


Fig. 2 Differential pore volume V' as a function of the pore diameter d of sample A

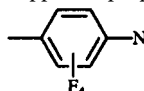
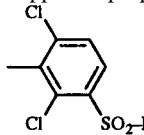
agreement with scanning electron microscopy (SEM) investigations, showing drastically different particle sizes between compounds A and C. The diameter of the particles in the former material is rather uniform, ranging from about 0.1 to 0.2 microns, while the high resolution SEM illustrations (Fig. 1) reveal large aggregates (>100 microns) for the latter material. Moreover, the surface areas measured for compounds A and B are essentially microporous [Table 1, micropore volume: $0.12 \text{ cm}^3 \text{ g}^{-1}$ (A), $0.24 \text{ cm}^3 \text{ g}^{-1}$ (B)]; furthermore, the Horvath-Kawazoe⁷ differential pore volume

plots showed a narrow micropore size distribution with an average diameter of 5 Å (Fig. 2). Finally, when the time of reaction for the preparation of A is changed (to 8 h), the material obtained (A') has an elemental analysis and spectroscopic data (UV/VIS, EXAFS-XANES, ³¹P MAS NMR, TGA, IR, etc.), identical to that of A (standard preparation time of 5 days). The only difference lies in the absence of notable microporosity, a property that appears after a prolonged reaction time, while the external surface areas are comparable for the two compounds (around $70 \text{ m}^2 \text{ g}^{-1}$).

At this stage, to get additional information about our series of supported porphyrins, their ability to catalyse the epoxidation of cyclooctene by PhIO was investigated (Table 2). The initial reaction rates measured for A–D are invariably lower (by a factor of *ca.* 4) than in the homogeneous system (Fig. 3). Surprisingly, similar reaction rates were obtained for compounds A and A', thus indicating that the microporous surface does not participate in the catalytic activity and that only the external surface of the catalyst particles is involved.

Subsequently, in order to investigate more thoroughly the arrangement of the porphyrin units on the surface of the solids, as well as their accessibility to substrates, the catalytic performances of the supported catalysts were compared to their related homogeneous precursors for the competitive hydroxylation of a mixture of alkanes of different sizes [*e.g.*, cyclododecane–cyclohexane (1 : 1)] with PhIO (Table 3). In homogeneous medium, for porphyrins 1A–1D, the hydroxylation rate for the C₁₂ cyclic alkane is higher than for the C₆

Table 2 Compared kinetics of the catalytic epoxidation of cyclooctene by PhIO, for supported porphyrins A–D and their homogeneous precursors

Catalyst		Initial reaction rate ^b	Yield ^c after 24 h/%
1A ^a	C ₆ H ₄ -P(O)(OEt) ₂	18	96
	Supported porphyrin A ^d	4.5	70
	Supported porphyrin A' ^e	4.5	67
1B ^a	C ₆ H ₄ -C ₆ H ₄ -P(O)(OEt) ₂	18	88
	Supported porphyrin B ^d	4.0	68
1C ^a	 -NH-C ₃ H ₆ -PO(OEt) ₂	22	98
	Supported porphyrin C ^d	6	90
1D ^a	 -SO ₂ -NH-C ₃ H ₆ -PO(OEt) ₂	26	98
	Supported porphyrin D ^d	6.5	96

^a Substituent at the *meso* position of the porphyrin. ^b Initial reaction rate = mol of epoxide (mol Mn porphyrin)⁻¹ min⁻¹; these values refer to the initial slope of the yield time plots. Conditions: molar ratio of catalyst : PhIO : cyclooctene = 1 : 10³ : 10⁵; 'equivalent concentration' of supported catalyst: 10⁻³ mol L⁻¹ in 1 mL of CH₂Cl₂ : CH₃CN (1 : 2). ^c Conditions: molar ratio of catalyst : PhIO : cyclooctene = 1 : 20 : 800; 'equivalent concentration' of supported catalyst: 10⁻³ mol L⁻¹ in 1 mL of CH₂Cl₂ : CH₃CN (1 : 2). ^d As defined in Scheme 2. Standard preparation time is 5 days. ^e Same protocol as for A, with a preparation time of 8 h.

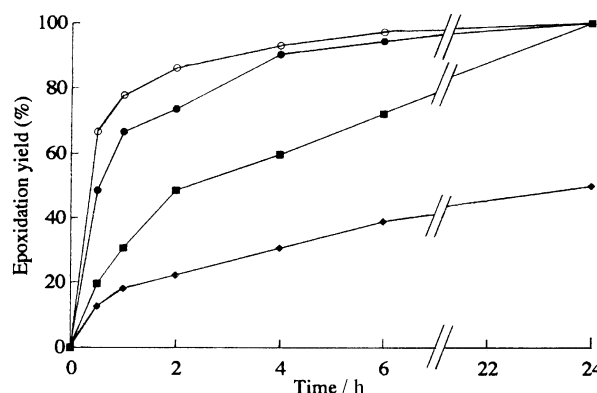
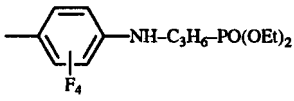
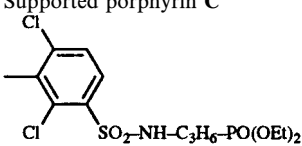


Fig. 3 Compared reaction rate curves for the epoxidation of cyclooctene by PhIO. Catalyst: (●) 1A, (◆) A, (○) 1C, (■) C.

Table 3 Competitive hydroxylation of a cyclododecane–cyclohexane mixture (1 : 1) for supported porphyrins **A–D**, and their homogeneous counterparts

Catalyst		Cyclododecanol : cyclohexanol ratio	Total yield per PhIO/% ^b
1A^a	C ₆ H ₄ -P(O)(OEt) ₂	2.3	13
	Supported porphyrin A^c	1.0	7
1B^a	C ₆ H ₄ -C ₆ H ₄ -P(O)(OEt) ₂	4.5	13
	Supported porphyrin B^c	1.0	8
1C^a		1.6	47
	Supported porphyrin C^c	0.4	27
1D^a		2.1	50
	Supported porphyrin D^c	0.4	46

^a Substituent at the *meso* position of the porphyrin. ^b Conditions: molar ratio of catalyst : PhIO : cyclododecane : cyclohexane = 1 : 20 : 400 : 400; 'equivalent concentration' of supported catalyst: 10⁻³ mol L⁻¹ in 1 mL of CH₂Cl₂; yields at 20 °C after 2 h. ^c As defined in Scheme. 2.

analogue, while for the supported porphyrins, a drastic change in the selectivity is observed, and cyclohexanol is now the major product formed in the hydroxylation reaction. This effect is particularly significant for **C** and **D**.

Discussion

It is apparent from these results that the nature of the linker between the porphyrin ring and the PO₃H₂ units has a strong effect on the texture of the supported catalysts. It is reasonable to think that this phenomenon might arise from differences in the rigidity (rigid phenyl or biphenyl rings *vs.* flexible aminopropyl chains) and polarity of the spacer. In order to know which of these two parameters is the most crucial, we have investigated the synthesis of the analogue of **1A**, in which the C₆H₄ spacer would be replaced by a C₆F₄ group; unfortunately, all attempts to prepare this compound were unsuccessful.

On the other hand, the orientation/disposition of the Mn porphyrins on the surface of the solids (also strongly related to the nature of the linker) is certainly the key feature responsible for the greater selectivity for cyclohexane over cyclododecane, observed in the hydroxylation test. If we suppose that the mechanism involved is the same for the homogeneous and supported catalysts, a possible explanation is to assume that the access of the bulky substrate to the catalytic sites is hindered, on account of steric constraints imposed by the phosphonate network. This would be in agreement with the results obtained for the hydroxylation of a second type of alkane mixture [adamantane–cyclohexane (1 : 1)]. Similarly, lower adamantanol : cyclohexanol ratios (from 4 to 2) are measured for supported porphyrins **A–D**, compared to those observed (>15) for the analogues in homogeneous medium, consistent with the higher reactivity of the tertiary CH groups of adamantane.

Taking into account the fact that these reactions take place at the surface of the solids, the contribution of the inorganic framework to this shape selectivity effect remains to be determined. In fact, the porphyrinic rings are tightly held together through zinc phosphonate blocks bound at the end of the spacers; these metal–PO₃ moieties consequently surround each of the catalytic sites. Could this result in a corrugated aspect of the surface of the heterogenised catalysts, making the access of bulky substrates (*i.e.*, cyclododecane and adamantane) to the Mn porphyrins more difficult? Detailed

local information about the structural environment of the catalytic sites would be necessary to confirm this hypothesis. However, these preliminary results give clear evidence of the important effect of the nature of the spacers present on the porphyrin backbone, on the structure and on the reactivity of the resulting supported catalysts. We are currently preparing manganese porphyrins with flexible spacers of variable length, in order to determine if better shape selectivities can be achieved by this strategy.

Experimental

The SEM experiments were carried out on a JEOL 6400F microscope. The BET (Brunauer–Emmet–Teller) surface areas and pore volume distributions were obtained from nitrogen adsorption isotherms measured with a conventional sorptometer. Samples were pretreated by heating up to 180 °C and evacuated for 6–8 h under reduced pressure. Surface areas were calculated using the BET equation and the external surfaces were evaluated from the *t*-plot analysis; to ensure that the preparations of the supported porphyrin were repeatable, we have checked, for each of them, that identical results were obtained from batch to batch. For the catalytic tests, yields were determined by GC, using internal standard methods. The characterisation of all the compounds was performed using previously described procedures.⁴ Porphyrins **1A** and **1C** were prepared as previously reported.⁴

Synthesis of porphyrin **1B**

4-Bromo-4'-formylbiphenyl⁸ was first acetalised with ethylene glycol. Then, to a stirred mixture of toluene (30 mL), diethyl phosphite (12.2 mL, 95 mmol), triethylamine (13.2 mL, 95 mmol) and 4-bromo-4'-(1'',3''-dioxolane-2''-yl)biphenyl (26.4 g, 86.5 mmol), a catalytic amount of tetrakis(triphenylphosphine)palladium(0) (5 g, 4.3 mmol) was added under a nitrogen atmosphere; the resulting mixture was stirred at 90 °C for 24 h. After cooling, the reaction medium was filtered on Celite and the filtrate was evaporated under reduced pressure. Afterwards, the crude product was stirred at ambient temperature for 8 h with 86.5 mL of 1 N sulfuric acid and 95 mL of THF. At the end of this period, CH₂Cl₂ (200 mL) was added and the organic layer was washed with saturated NH₄Cl solution, dried over MgSO₄ and evaporated. After flash chromatography of the residue on a silica gel column (eluent: 50% hexane in ethyl acetate), 4-

diethoxyphosphoryl-4'-formylbiphenyl was obtained in 80% yield as a white solid: mp 71 °C; ^1H NMR (200 MHz, CDCl_3 , δ): 1.35 (6 H, t, Et); 4.15 (4 H, d of q, Et); 7.75 (4 H, m, C_6H_4); 7.95 (4 H, m, C_6H_4); 10.1 (1 H, s, CHO); MS: m/z 318 (M^+); anal. calcd for $\text{C}_{17}\text{H}_{19}\text{O}_4\text{P}$: C, 64.15; H, 6.02; P, 9.73; found: C, 64.02; H, 6.00; P, 9.53.

A solution of 2 g (6.3 mmol) of the above aldehyde and 0.44 mL (5.7 mmol) of pyrrole in 30 mL of propionic acid was refluxed in a flask protected from light, at 150 °C for 1.5 h. The mixture was evaporated to dryness and after flash chromatography of the residue on a neutral alumina column (eluent 1.5% methanol in dichloromethane), the resulting dark oil was crystallised in acetonitrile to give the free-base form of **1B** in 32% yield as violet crystals: mp 293 °C; ^1H NMR (200 MHz, CDCl_3 , δ): -2.6 (2 H, s, NH); 1.40 (24 H, t, Et); 4.25 (16 H, d of q, Et); 8.0 and 8.3 (16 H, 2d, C_6H_4 , $^3J_{\text{HH}} = 8$ Hz), 8.05 (16 H, m, C_6H_4); 8.8 (8 H, s, CH-py); ^{31}P NMR (81 MHz, CDCl_3 , δ): 18.2; FAB-MS (*m*-nitrobenzyl alcohol matrix): m/z 1463 ($\text{M} + \text{H}^+$); UV/VIS (CH_2Cl_2): λ_{max} (10^{-3} ϵ) 422 nm (Soret, 810 $\text{L mol}^{-1} \text{cm}^{-1}$), 519 (34), 553 (28), 591 (15), 647 (14); anal. calcd for $\text{C}_{84}\text{H}_{82}\text{N}_4\text{O}_{12}\text{P}_4$: C, 68.94; H, 5.65; N, 3.83; found: C, 68.48; H, 5.71; N, 3.78. **1B** was obtained by metallation of its free-base form, using manganese(II) acetate according to previously described procedures.⁹ FAB-MS (*m*-nitrobenzyl alcohol matrix): m/z 1515 ($\text{M} - \text{Cl}^+$); UV/VIS (CH_2Cl_2): λ_{max} (10^{-3} ϵ) 479 nm (Soret, 173), 584, 621. The Mn:P and Mn:Cl ratios measured by energy dispersive X-ray spectroscopy (EDXS) were in good agreement with the expected values. **1B** was converted into its acidic PO_3H_2 form using bromotrimethylsilane, as reported in the literature.¹⁰

Synthesis of porphyrin 1D

meso-5,10,15,20-Tetrakis-(2,6-dichlorophenyl)porphyrin¹¹ (H_2TDCPP) was chlorosulfonated as previously described.¹² A flask was charged with 50 mL of freshly distilled THF and 25 μL of dimethoxypropane; the solution was purged with argon for 1 h. Diethyl-3-aminopropylphosphonate⁴ (1.14 g, 5.85 mmol) and anhydrous pyridine (315 μL , 3.9 mmol) were then added and the solution was purged again with argon for 1 h. Finally, 0.5 g (0.39 mmol) of the chlorosulfonated porphyrin ($\text{H}_2\text{TDCPPm-SO}_2\text{Cl}$) was introduced and the reaction mixture was stirred at room temperature for 30 min. After filtration and evaporation of the solvents, the crude product was dissolved in dichloromethane and washed with a saturated NaHCO_3 solution. The organic layer was dried over magnesium sulfate and evaporated; the resulting product was purified by chromatography on a silica gel column (eluent: 3% ethanol in dichloromethane) to give the free-base form of **1D** as a violet solid in 55% yield. ^1H NMR (200 MHz, CDCl_3 , δ): -2.5 (2H, s, NH); 1.2 (24 H, t, Et); 1.8 (16 H, m, $\text{CH}_2\text{CH}_2\text{P}$); 3.3 (8 H, m, CH_2N); 4.05 (16 H, d of q, Et); 6.5 (4 H, bs, NH_2SO_2); 7.9 (4 H, d, $\text{C}_6\text{H}_2\text{Cl}_2$, $^3J_{\text{HH}} = 8.5$ Hz); 8.55 (4

H, d, $\text{C}_6\text{H}_2\text{Cl}_2$, $^3J_{\text{HH}} = 8.5$ Hz); 8.65 (8 H, s, CH-py); FAB-MS (*m*-nitrobenzyl alcohol matrix): m/z 1919 ($\text{M} + \text{H}^+$); UV/VIS (CH_2Cl_2): λ_{max} (10^{-3} ϵ) 419 nm (Soret, 620 $\text{L mol}^{-1} \text{cm}^{-1}$), 513 (33), 589 (13); anal. calcd for $\text{C}_{72}\text{H}_{86}\text{N}_8\text{O}_{20}\text{P}_4\text{Cl}_{18}\text{O}_4$: C, 45.04; H, 4.53; N, 5.84; found: C, 44.80; H, 4.63; N, 5.82. **1D** was obtained by metallation of its free-base form, using manganese(II) acetate according to previously described procedures.⁹ FAB MS (*m*-nitrobenzyl alcohol matrix) m/z 1971 ($\text{M} - \text{Cl}^+$); UV/VIS (CH_2Cl_2): λ_{max} (10^{-3} ϵ) 467 nm (Soret, 110 $\text{L mol}^{-1} \text{cm}^{-1}$), 565 (5), 661 (6). The Mn:P, Mn/S and Mn:Cl ratios measured by EDXS were in good agreement with the expected values. **1D** was converted into its acidic PO_3H_2 form using bromotrimethylsilane, as reported in the literature.¹⁰

The heterogenization of porphyrins **1A–1D** was performed following the same protocol; typically, a mixture of 250 mg of the desired porphyrin (in its PO_3H_2 acidic form) and 100 equivalents of zinc nitrate were stirred and refluxed in methanol for 5 days. The resulting zinc phosphonate (**A–D**, quantitative yield) was washed with methanol, water and acetone, then filtered and dried at room temperature.

References

- 1 For recent reviews about the chemistry of phosphonates, see for example: A. Clearfield, *Curr. Opin. Solid State Mater. Sci.*, 1996, **1**, 268; G. Alberti, in *Comprehensive Supramolecular Chemistry*, ed. G. Alberti and T. Bein, Pergamon Press, New York, 1996, vol. 7, p. 151.
- 2 F. Fredouel, V. Penicaud, M. Bujoli-Doeuff and B. Bujoli, *Inorg. Chem.*, 1997, **36**, 4702 and references therein.
- 3 See for example: A. Corma, M. Iglesias, C. del Pino and F. Sanchez, *J. Chem. Soc., Chem. Commun.*, 1991, 1253; J. M. Andersen and A. W. S. Currie, *Chem. Commun.*, 1996, 1543; A. W. S. Currie and J. M. Andersen, *Catal. Lett.* 1997, **44**, 109; R. Y. V. Subba, D. E. De Vos, T. Bein and P. A. Jacobs, *Chem. Commun.*, 1997, 355.
- 4 D. Deniaud, B. Schöllhorn, D. Mansuy, J. Rouxel, P. Battioni and B. Bujoli, *Chem. Mater.*, 1995, **7**, 995.
- 5 P. Battioni, E. Cardin, M. Louloudi, B. Schöllhorn, G. A. Spyroulias, D. Mansuy and T. G. Traylor, *Chem. Commun.*, 1996, 2037.
- 6 O. Bortolini, M. Ricci, B. Meunier, P. Friant, I. Ascone and J. Goulon, *New J. Chem.*, 1986, **10**, 39.
- 7 G. Horvath and K. Kawazoe, *J. Chem. Eng. Jpn.*, 1983, **16**, 470.
- 8 P. K. Dhal, *Macromol. Rep.*, 1992, **A29**, 39.
- 9 R. D. Jones, F. Basolo and D. A. Summerville, *J. Am. Chem. Soc.*, 1978, **100**, 4416.
- 10 C. E. Mc Kenna, M. T. Higa, N. H. Cheung and M. C. Mc Kenna, *Tetrahedron Lett.*, 1977, 155.
- 11 C. L. Hill and M. M. Williamson, *J. Chem. Soc., Chem. Commun.*, 1985, 1228.
- 12 A. M. Da Rocha Gonsalves, R. A. W. Johnstone, M. M. Pereira, A. M. P. De SantAna, A. C. Serra, A. J. F. N. Sobral and P. A. Stocks, *Heterocycles*, 1996, **43**, 829.

Received in Orsay, France, 16th June 1997; Revised manuscript received 12th January, 1998; Paper 7/09254G